Energy Management of Microgrid in Grid-Connected and Stand-Alone Modes

Quanyuan Jiang, *Member, IEEE*, Meidong Xue, and Guangchao Geng, *Student Member, IEEE*

***Abstract*—There are two operation modes of microgrids: grid-connected mode and stand-alone mode. Normally, a microgrid will be connected to the main grid for the majority of time, i.e., operates in the grid-connected mode. In the stand-alone mode, a microgrid is isolated from the main grid; the highest priority for microgrids is to keep a reliable power supply to customers instead of economic benefits. So, the objectives and energy management strategies are different in two modes. In this paper, a novel double-layer coordinated control approach for microgrid energy management is proposed, which consists of two layers: the schedule layer and the dispatch layer. The schedule layer obtains an economic operation scheme based on forecasting data, while the dispatch layer provides power of controllable units based on real-time data. Errors between the forecasting and real-time data are resolved through coordination control of the two layers by reserving adequate active power in the schedule layer, then allocating that reserve in the dispatch layer to deal with the indeterminacy of uncontrollable units. A typical-structure microgrid is studied as an example, and simulation results are presented to demonstrate the performance of the proposed double-layer coordination control method in both grid-connected mode and stand-alone mode.**

***Index Terms*—Double-layer coordinated control, energy management, grid-connected mode, microgrid, optimization methods, power control, stand-alone mode.**

NOMENCLATURE

Variables:	
P, Q	Active and reactive power of controllable units.
U	Operation state of controllable units.
E	Energy level of ESS.
V_e, V_f	Real and imaginary part of the bus voltage.
Subscripts:	
G	Dispatchable DG unit.
I	Non-dispatchable DG unit.
$S+, S-$	Charging/discharging state of the ESS.
$grid+, grid-$	Buying from/selling to the main grid.
LI, LN	Interruptible load/normal load.
*	Sign of operation states changed.
Symbols:	
θ	Set of variables.
θ_T	Time set.
c_L	Price of load serving.
K_{OM}	Operation and maintenance costs of dispatchable DG unit.
c_G^{on}	Startup cost of DG unit.
c_{Si+}, c_{Si-}	Charging/discharging cost of ESS.
c_S^{cycle}	Cost of ESS for periodic duty.
c_{grid+}, c_{grid-}	Price of power buying from/selling to the main grid.
K_L	Punishment cost for load shedding.
L_G	Segments of dispatchable DG power.
B^k	Initial power of piece k.
A^k	Fuel cost for initial power of piece k.
F^k	Fuel cost for unit power of piece k.
D^k	Power of dispatchable DG in piece k.
v^k	Sign of piece k.
η_c, η_d	Charging/discharging efficiency of ESS.
ΔT	Time step.
$\underline{E}, \overline{E}$	Limit of energy level.
$\underline{P}, \overline{P}$	Limit of power.
S_N	Nominal power/inverter capacity.
R	Power reserve coefficient.
a, b, c	Parameters of DG unit's fuel cost.
$\hat{P}$	Power reference of controllable units.
λ	Power factor.
r	Power allocation coefficient.

Manuscript received September 07, 2012; revised December 16, 2012; accepted January 27, 2013. Date of publication March 07, 2013; date of current version July 18, 2013. This work was supported by the National High Technology Research, Development Programming and National Natural Science Foundation of China (2009AA05Z221, 2011AA05A113, 51207140). Paper no. TPWRS-01032-2012.

The authors are with the College of Electrical Engineering, Zhejiang University, Hangzhou 310027, China (e-mail: jqy@zju.edu.cn; xuemd2006@163.com; genggc@gmail.com).

Color versions of one or more of the figures in this paper are available online at http://ieeexplore.ieee.org.

Digital Object Identifier 10.1109/TPWRS.2013.2244104

I. Introduction

MICROGRIDS are the systems that integrate distributed generation (DG) units, energy storage systems (ESS) and controllable loads on a low voltage network which can operate in either grid-connected mode or stand-alone mode [1], [2]. In the grid-connected mode, the microgrid adjusts power balance of supply and demand by purchasing power from the main grid or selling power to the main grid to maximize operational benefits. In the stand-alone mode, the microgrid is separated from the upstream distribution grid, and aims to keep a reliable power supply to customers using DG bids [3]. To alleviate the power fluctuations of non-dispatchable DG units, various control schemes are used in microgrids, including power regulation of each dispatchable DG unit, charging and discharging of ESS, and load shedding [4]. The control strategy for units within a microgrid can be a grid-following control strategy based on a voltage-sourced converter (VSC) [5]–[9] or a grid-forming control strategy based on droop control [10], [11]. A microgrid usually requires an energy management strategy—assigning active and reactive power references, and ensuring cooperation between the controllable units to achieve stable and economic operation [12], [13].

According to the latest research, the objective of energy management of microgrid is to minimize microgrid's operating costs such as fuel costs, operating maintenance costs, and purchased cost of electricity from the main grid. In [3], an energy management approach is proposed based on two market policies only considering power balance. Security is not considered in the microgrid operation. In [14] and [15], the charging/discharging power of energy storage system is decided based on the heuristics. It causes the power regulation is independent in each time-step and no coordination with other units. In [16], an optimal power flow problem is applied to energy management only based on the current information. However, without coordination of the controllable units in a long-time optimization, the power of DG units will fluctuate as they follow wind power. In [17], Operation optimization of microgrid is simplified into a multiple-time optimization problem with an emphasis on energy storage system. It can only give a day-ahead operation scheme, but no consideration of the RES power fluctuation and the related regulation method. A similar multiple-time optimization problem is proposed in [18] as the top layer. The RES power fluctuation is smoothed by the build-in energy storage in component-layer. But there is no countermeasure that shows the coordination of the two layers when the power fluctuation is over the capacity of build-in energy storage. Otherwise, the build-in energy storage must be large enough to handle any fluctuation; in that case the energy storage system in top layer is meaningless. In [19], a scheme was developed based on the behavior of N time periods ahead, with the optimization problem rolling over time horizons resulting in a modification of generator behavior over the rest of time periods. A common disadvantage of the methods described earlier is not to take into account the comprehensive aspects of energy management, such as difference between grid-connected mode and stand-alone mode, coordination of controllable units in long-time, influence on voltage and power flow, power regulation caused by forecasting error of intermittent resources.

The emphasis of this paper is energy management of microgrid in grid-connected and stand-alone modes based on a double-layer coordinated control approach, consisting of the schedule layer and the dispatch layer. The schedule layer provides an economical operation scheme—including state and power of controllable units—based on the look-ahead multi-step optimization, while the dispatch layer follows the schedule layer by considering power flow and voltage limits. So that the economic benefit and technical constraints on long-time operation are considered. The key point of the proposed approach is in the coordination of the two layers for dealing with the indeterminacy between forecasting data and real-time data which makes up for the influence of forecasting errors on multi-step optimization problem. Also the difference of two operation modes is considered, especially on the power reserve and power regulation.

This paper is organized as follows: Section II describes the proposed approach in brief, followed by models in both grid-connected mode and stand-alone mode. The coordination method of the proposed approach is discussed in Section III. Simulation results for both grid-connected mode and stand-alone mode are given in Section IV. Section V concludes this paper.

II. Energy Management Model

Energy management of microgrid is divided into grid-connected mode and stand-alone mode for the different operation requirements.

A. Grid-Connected Mode

Due to connecting to the main grid, load demand can be met all the time. So the operation objective of microgrids is to maximize revenues according to DG bids and market price. For energy saving and environmental benefit, the wind and solar generation power are totally used. The requirements of voltage and power flow are taken into account at the same time, especially at the point of common coupling (PCC). Above operation requirements are achieved by a double-layer coordinated control approach, which includes schedule layer and dispatch layer.

The schedule layer is maximizing revenues over a given time horizon by finding the best possible control sequence of controllable units, taking into account market prices, forecasting power of non-dispatchable DG units, and load level. By piecewise linearization of dispatchable DG units' fuel costs, the energy management problem can be formulated as a mixed-integer linear problem (MILP).

The control variables include active power and operation state of ESS and dispatchable DG units, active power exchanged with the main grid over the given time horizon. Others are state variables:

$$x_s = \begin{cases} \text{Control variables :} \\ P^t_{Gi}, P^t_{Si+}, P^t_{Si-}, P^t_{grid+}, P^t_{grid-}, U^t_{Gi}, U^t_{Si+}, U^t_{Si-}, \\ U^t_{grid+}, U^t_{grid-} \\ \text{State variables :} \\ D^{t,k}_i, v^{t,k}_i, U^t_{Gi_*}, E, U^t_{Si_*} \end{cases}$$

The objective function is given as follows:

$$\max \quad f(x_s) = f_L(x_s) - f_G(x_s) - f_S(x_s) - f_{grid}(x_s) \tag{1}$$

$$f_L(x_s) = \sum_{t\in\theta_T} \sum_{i\in\theta_{LN,LI}} c_L^t P_{Li}^t \tag{2}$$

$$f_G(x_s) = \sum_{t\in\theta_T} \sum_{i\in\theta_G} \left[U_{Gi}^t A_i^1 + \sum_{k=1}^{L_{Gi}} \left(F_i^k D_i^{t,k} \right) + K_{OMi} P_{Gi}^t + c_{Gi}^{on} U_{Gi^*}^t \right] \tag{3}$$

$$f_S(x_s) = \sum_{t\in\theta_T} \sum_{i\in\theta_S} \left(c_{Si+} P_{Si+}^t + c_{Si-} P_{Si-}^t + c_{Si}^{cycle} U_{Si^*}^t \right) \tag{4}$$

$$f_{grid}(x_s) = \sum_{t\in\theta_T} \left(c_{grid+}^t P_{grid+}^t - c_{grid-}^t P_{grid-}^t \right) \tag{5}$$

where f_L is the revenue from serving loads. f_G is the cost of dispatchable DG units, including fuel costs, operation and maintenance costs, and startup costs. f_S is the cost of the ESS, and f_{grid} is the revenue obtained from buying and selling power to the main grid.

Power reserve to compensate forecasting errors is set in (6) at each time-step. Power reserve coefficient R depends on forecasting accuracy of uncontrollable units' power and load level, which leaves adequate power margin of controllable units to deal with real-time power fluctuation owing to forecasting error. For large reserve power is non-economic, it is set to lower value at beginning and enlarged when the operation scheme fails:

$$\overline{P_{grid+}} - P_{grid+}^t + P_{grid-}^t + \sum_{i\in\theta_G} \left(U_{Gi}^t \overline{P_{Gi}} - P_{Gi}^t \right) \geq R\% \left(\sum_{i\in\theta_{LN,LI}} P_{Li}^t + \sum_{i\in\theta_I} P_{Ii}^t \right). \tag{6}$$

Power of the dispatchable DG units is defined in (7)–(9) after piecewise linearization. Because the quadratic curve of fuel cost is changed to several line segments, the control problem is relatively easy to solve as a MILP:

$$P_{Gi}^t = U_{Gi}^t B_{Gi}^1 + \sum_{k=1}^{L_{Gi}} D_{Gi}^{t,k} \tag{7}$$

$$\sum_{j=k+1}^{L_{Gi}} v_i^{t,j} \leq \frac{D_i^{t,k}}{B_i^{k+1} - B_i^k} \leq \sum_{j=k}^{L_{Gi}} v_i^{t,j} \tag{8}$$

$$\sum_{k=1}^{L_{Gi}} v_{Gi}^{t,k} = U_{Gi}^t. \tag{9}$$

The relationship of the ESS energy level between two time-steps, which considers conversion losses, is represented in (10) and (11):

$$E_i^t - E_i^{t-1} = \Delta T \left(\eta_c P_{Si+}^{t-1} - \frac{P_{Si-}^{t-1}}{\eta_d} \right) \tag{10}$$

$$\underline{E_i} \leq E_i^t \leq \overline{E_i}. \tag{11}$$

Constraints (12) guarantee the microgrid either receiving power or sending power to main grid. This also applies to charging and discharging power of ESS in (13):

$$U_{grid+}^t + U_{grid-}^t \leq 1 \tag{12}$$

$$U_{Si+}^t + U_{Si-}^t \leq 1. \tag{13}$$

There are also basic power balance equations, power limits and ramp limits of controllable units, maximum startup time of dispatchable DG units to be considered in the schedule layer.

At a given time step t, the operating state and planned power of controllable units are determined by the schedule layer. Power controlled by the dispatch layer will alleviate the power fluctuations of non-dispatchable DG units in response to any forecasting error of data in the schedule layer, and optimize voltage and power flow at the same time. The objective is to minimize cost of power regulation with a penalty function to follow the economic operation scheme in the schedule layer; namely, the operating state is unchanged and power is fixed according to the planned value. The energy management problem is formulated as a non-linear problem (NLP).

Although the active power of non-dispatchable DG units is uncontrollable and completely used, the reactive power participates in voltage regulation:

$$x_d = \begin{bmatrix} P_{Gi}, P_{Si}, P_{grid} \\ Q_{Gi}, Q_{Si}, Q_{grid}, Q_{Ii} \\ V_{ei}, V_{fi} \end{bmatrix}.$$

In the objective, f_G, f_S, f_{grid} are the operating costs of the DG units, the ESS, and transactions with the main grid and μ is a penalty factor:

$$\min \quad f(x_d) = f_G(x_d) + f_S(x_d) + f_{grid}(x_d) \tag{14}$$

$$f_G(x_d) = \sum_{i\in\theta_G} \left[a_i P_{Gi}^2 + b_i P_{Gi} + c_i + \mu_{Gi} (P_{Gi} - \hat{P}_{Gi})^2 \right] \tag{15}$$

$$f_S(x_d) = \sum_{i\in\theta_S} \left[c_{Si} P_{Si} + \mu_{Si} (P_{Si} - \hat{P}_{Si})^2 \right] \tag{16}$$

$$f_{grid}(x_d) = c_{grid} P_{grid} + \mu_{grid} (P_{grid} - \hat{P}_{grid})^2. \tag{17}$$

Constraint (18) is the nominal power/inverter capacity of all units. Security constraints are set in the model, including voltage limits, transmission power limits, power flow equations and power limits of the controllable units:

$$\sqrt{P_i^2 + Q_i^2} \leq S_{Ni}. \tag{18}$$

Considering the influences on the main grid, power exchanged with the microgrid and the power factor at PCC is controlled in (19) and (20):

$$\underline{P_{grid}} \leq P_{grid} \leq \overline{P_{grid}} \tag{19}$$

$$\underline{\lambda}^2 \leq \frac{P_{grid}^2}{P_{grid}^2 + Q_{grid}^2} \leq 1. \tag{20}$$

B. Stand-Alone Mode

When the main grid is gone, the highest priority is to keep a reliable power supply to customers instead of economic benefits. So the operation objective of microgrids is to maximize satisfaction rate of load with minimum operation cost. It means that the wind and solar generation power should be totally used to make up the lack of electricity and part of load could be cut off to balance power when necessary. The double-layer coordinated control approach is suitable for stand-alone mode.

In schedule layer:

$$x_s = \begin{bmatrix} \text{Control variables :} \\ P_{Gi}^t, P_{Si+}^t, P_{Si-}^t, U_{Gi}^t, U_{Si+}^t, U_{Si-}^t, U_{Li}^t \\ \text{State variables :} \\ D_i^{t,k}, v_i^{t,k}, U_{Gi^*}^t, E, U_{Si^*}^t \end{bmatrix}$$

U_{Li}^t is a control variable to determine the operation state of interruptible load. This is a demand side management that consumers get power from microgrid instead of the main grid. The consumers are divided in two parts: normal load and interruptible load. The former gives priority to power supply. Microgrid obtains the right of load shedding from the latter by a high compensation to balance power, i.e., a penalty for load shedding which is more than generation cost to avoid that happens.

In the objective, f_G, f_S are the same as that in grid-connected mode and f_L is the penalty function for load shedding:

$$\min \quad f(x_s) = f_G(x_s) + f_S(x_s) + f_L(x_s) \tag{21}$$

$$f_L(x_s) = \sum_{t\in\theta_T} \sum_{i\in\theta_{LI}} K_L(1 - U_{Li}^t) P_{Li}^t \tag{22}$$

and constraint (23) limits the time of load shedding to avoid frequent load cutoffs in a short period of time:

$$\sum_{j=0}^{m} U_{Li^*}^{t+j} \le 1. \tag{23}$$

Without the power support of main grid, the power regulation capability is limited by ramp constraint ΔP_{Gi} of each DG unit. Although a unit operates with large range of power adjustment $[0, \overline{P_{Gi}}]$, the output power at next time-step is regulated in $[P_{Gi}^{t-1} - \Delta P_{Gi}, P_{Gi}^{t-1} + \Delta P_{Gi}]$. The practical adjustable power is determined by the power range and ramp limit of DG units collectively as shown in Fig. 1:

$$\sum_{i\in\theta_G} \left[\min\left(U_{Gi}^t \overline{P_{Gi}}, P_{Gi}^{t-1} + \Delta P_{Gi}\right) - P_{Gi}^t\right] \ge R\% \left(\sum_{i\in\theta_{LN}} P_{Li}^t + \sum_{i\in\theta_{LI}} U_{Li}^t P_{Li}^t + \sum_{i\in\theta_I} P_{Ii}^t\right). \tag{24}$$

In dispatch layer, interruptible load is still one of control variables because load shedding is an essential mean to deal with the sudden power decrease of non-dispatchable DG units:

$$x_d = \begin{bmatrix} P_{Gi}, P_{Si}, P_{Li} \\ Q_{Gi}, Q_{Si}, Q_{Ii} \\ V_{ei}, V_{fi} \end{bmatrix}.$$

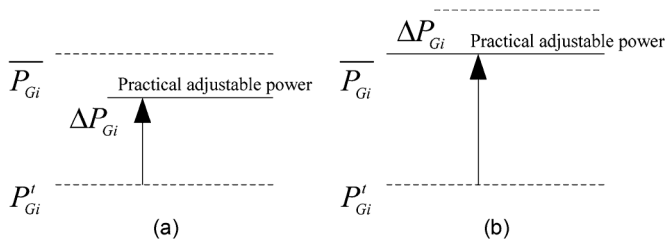

Fig. 1. Adjustable power considered in stand-alone mode.

In the objective, f_G, f_S are the same as that in grid-connected mode and $\hat{P}_{Li}$ is the load level after regulation of schedule layer:

$$\min \quad f(x_d) = f_G(x_d) + f_S(x_d) + \sum_{i\in\theta_{Li}} K_L(\hat{P}_{Li} - P_{Li}). \tag{25}$$

Except constraints about the grid such as (19) and (20), others are the same in both of the two modes.

Two layers of programming can be solved independently by CPLEX [20] but the results must be interrelated. The aim of the dispatch layer is to ensure the safety and stability of operations by adjusting power of the controllable units. If deviation from the planned value is excessive, the usefulness of the schedule layer is lost. Therefore, the power threshold is set to check feasibility. The power threshold of the dispatchable DG includes ramp constant and largest deviation from planned value:

$$\begin{cases} \overline{P_{Gi}^t} = \min\left(P_{Gi}^{t-1} + \Delta P_{Gi}\Delta T, P_{Gi}^t + \overline{P_{Gi}} \cdot r\right) \\ \underline{P_{Gi}^t} = \max\left(P_{Gi}^{t-1} - \Delta P_{Gi}\Delta T, P_{Gi}^t - \overline{P_{Gi}} \cdot r\right) \end{cases}. \tag{26}$$

For the ESS, the level of energy storage should also be considered:

$$\begin{cases} \overline{P_{Si}^t} = \min\left(P_{Si}^{t-1} + \Delta P_{Si}\Delta T, P_{Si}^t + \overline{P_{Si}} \cdot r, \left(E_i^{t-1} - \underline{E_i}\right) \cdot \eta_D / \Delta T\right) \\ \underline{P_{Si}^t} = \max\left(P_{Si}^{t-1} - \Delta P_{Si}\Delta T, P_{Si}^t - \overline{P_{Si}} \cdot r, \left(E_i^{t-1} - \overline{E_i}\right) / (\eta_C \cdot \Delta T)\right) \end{cases}. \tag{27}$$

Although the dispatch layer focuses on a given time step, it strictly follows the technical limits of dynamic change, ramp constant and limit of energy level. To minimize operating costs, the power allocation coefficient r is related to incremental cost and adjustable margin. Power allocation coefficient is not only the largest deviation, but also the weight of power distribution in smoothing power fluctuation.

III. Double-Layer Coordination Control

The time steps in the schedule layer are of the whole time horizon, looking N time steps into the future. For each time-step, the schedule layer determines the optimal control sequence—including the operation state and planned power of controllable units—based on the look-ahead multi-step optimization. At each time step of the schedule layer, the dispatch layer adjusts the power of controllable units based on operation state to optimize power flow and regulate voltage. As the time step moves to $t + i$, power flow optimization is carried out again by the dispatch layer. Note that there is a self-adjusting process built in both the schedule and the dispatch layer. When

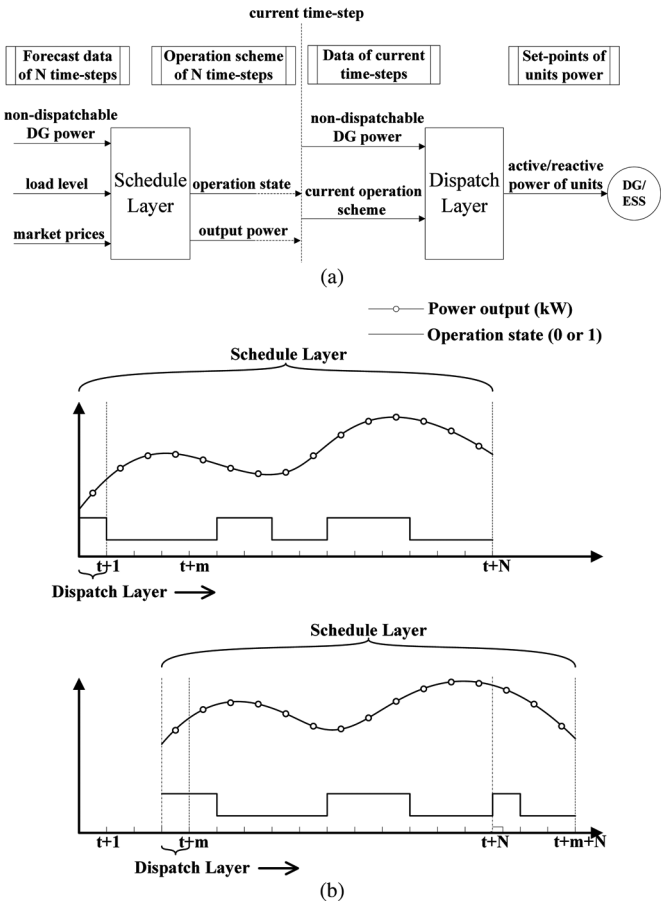

Fig. 2. Visualization of double-layer coordination. (a) Data stream. (b) Time stream.

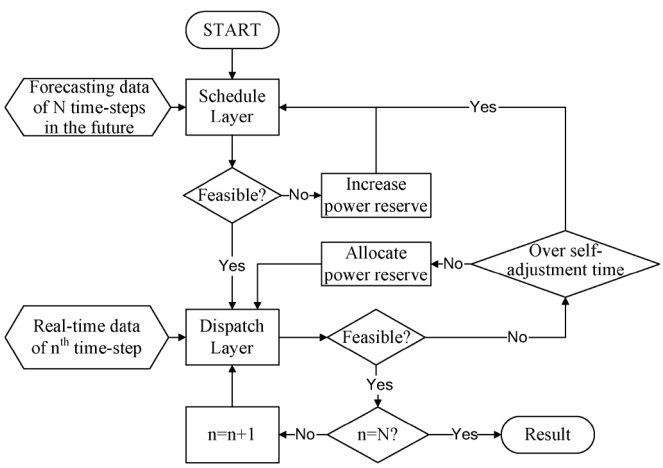

Fig. 3. Flowchart of double-layer coordination.

optimization fails in the dispatch layer, a new control sequence is made using the initial state at the step where the failure occurs (e.g. time-step $t+m$) and data of N time steps in the future. Moreover, the remaining control sequence (from time-step $t+m$ to $t+N$) will be updated. This concept is displayed in Fig. 2.

This control concept is suited for microgrid energy management because it allows a prediction when dispatchable DG is required. By partly feeding electricity into the ESS and releasing it over time at the highest level of demand, dispatchable DG units can operate stably and efficiently. On the other hand, the control algorithm is aware of the variation tendencies of the non-dispatchable DG power and of when the ESS will reach its upper/lower energy levels. Consequently, power of the DG units and of the ESS is regulated ahead of time, balancing the required increment/curtailment for future time steps and fixing any forecasting errors at future time steps when they occur.

The double-layer optimization procedure is as follows (shown in Fig. 3):

Step 1) Initialize time step $n = 1$ and get initial state of all units.

Step 2) Predict control sequence (operation state and planned power over all time steps) of controllable units based on forecasting data for a horizon of N time steps in the future using the schedule layer model.

Step 3) Check the result of *Step 2*. If there is no change in the control sequence of the nth step after adjustment of *Step 7*, relax the power reserve by enlarging reserve power coefficient R and go to *Step 2*. Otherwise, go to *Step 4*.

Step 4) Following completion of the nth step, power flow is optimized to get the real-time power of units according to real-time data using the dispatch layer model.

Step 5) Check the result of *Step 4*. If security constraints are not met, or power is over the technical and economic limits, go to *Step 6*. Otherwise, go to *Step 8*.

Step 6) First, increase the penalty factor to enforce controllable units following the control sequence, and adjust reserve power by the power allocation coefficient r according to incremental cost and adjustable margin in the dispatch layer. If self-adjustment of the dispatch layer does not work, go to *Step 7*. Otherwise, go to *Step 8*.

Step 7) Retrieve the state of all units in the $n-1$th step as the initial state, then return to *Step 2*.

Step 8) Record the scheme for the nth step. If $n < N$, then set $n = n+1$ and go to *Step 4*. Otherwise, the optimization is finished.

Forecasting data plays an important role in the schedule layer, especially for forecasting error in the power produced from non-dispatchable DG units. This error is known as power indeterminacy. The proposed coordination method handles power indeterminacy of non-dispatchable DG units by the coordination of the two layers. The schedule layer reserves adequate active power, which is then allocated in the dispatch layer to adjust the balance of supply and demand. The reserve is the total power between the upper limit and the planned value of all controllable units, so each DG unit has a different adjustable margin. The significance of the control sequence in the dispatch layer is based on the cooperation of controllable units in a long-time scale, and may not be optimal over shorter time scales. If the resulting control sequence is infeasible in the dispatch layer, controllable units with a lower incremental cost and larger adjustable margin are scheduled by adjusting power allocation coefficient r in the dispatch layer to smooth power fluctuation. If self-adjustment

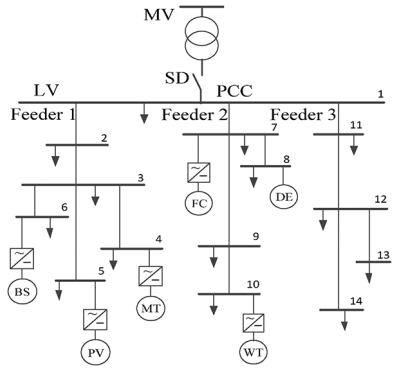

Fig. 4. Typical microgrid.

TABLE I
COMPONENT INFORMATION

Type		DE	MT	FC	BS	PV	WT
Output Limit (kW)	upper	60.00	75.00	80.00	90.00	200	250
	lower	11.11	12.74	14.00	30.00	—	—
Climbing Limit (kW/h)	upper	240	280	170	400	—	—
	lower	240	280	170	400	—	—

of the dispatch layer fails, a new control sequence will be made using that moment as the initial state. If the new control sequence fails again, enlarging the reserve power coefficient R ensures there is a more adjustable margin left for dealing with power indeterminacy.

IV. CASE STUDIES

The system setup used for the simulation in this paper is shown in Fig. 4, and consists of a group of radial feeders which could be part of a distribution system [3], [21], [22].

There is a single point of connection to the utility called the point of common coupling. Feeders 1 and 2 have sensitive loads which must be supplied during all events. The feeders also have non-dispatchable DG units consisting of a photovoltaic (PV) unit and a wind turbine (WT) unit, as well as dispatchable DG consisting of a fuel cell (FC), a micro turbine (MT), a diesel engine (DE), and ESS consisting of battery storage (BS). The third feeder has only traditional loads. There is a static switch (SD) in the PCC which can island the microgrid from the utility. Fuel inputs are needed only for the DE, FC, and MT units, as the WT and PV units do not require fuel. To serve the load demand, one or more of the PV, WT, DE, MT, or FC units can directly produce electrical power.

Each component of the microgrid system is separately modeled based on its characteristics and constraints (see Table I). The cost of each DG unit is fitted by changing the system parameters to reflect efficiency of the engines. Taking FC as an example in Fig. 5, piecewise linearization is used in the schedule layer and polynomial fitting is used in the dispatch layer to make problem solvable; however this does not significantly change the results.

All loads contain household and industry components, and a statistical investigation and analysis of typical demand curves [23] is provided in Fig. 6(a). Take a single day as an example, dividing it into 288 periods with 5 min as an interval. Load curves,

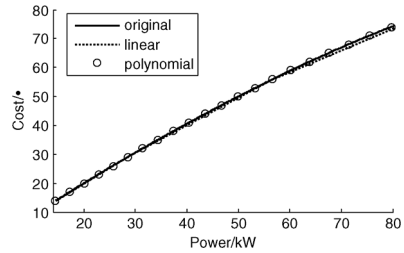

Fig. 5. Fuel cost of the FC unit.

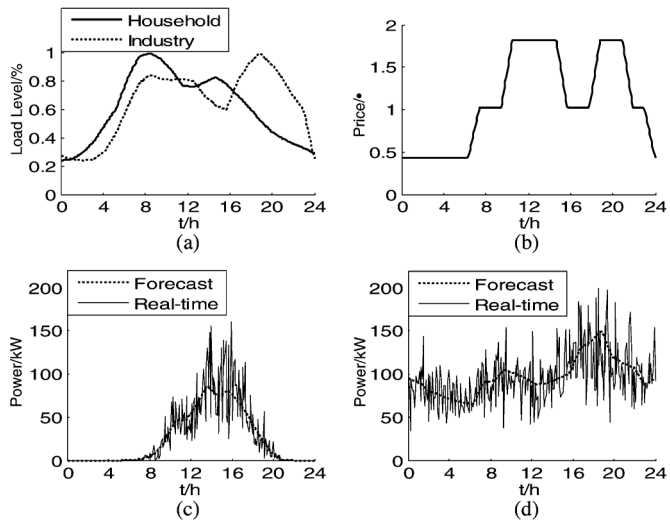

Fig. 6. Data for models. (a) Load curve. (b) Market price. (c) Power of PV unit. (d) Power of WT unit.

market prices, and the forecasting power from PV and WT units are shown in Fig. 6. The market prices reflect peak and valley loads of the main grid. Prices are high when power is lacking at peak load, and lower at valley load. Forecasting data (dotted line) and real-time data (solid line) for PV and WT units are provided in Fig. 6(c) and 6(d). The stochastic variables are assumed to follow a beta distribution [24], with forecasting values as the expected values.

In order to analyze and compare performance of the microgrid system in different situations, two cases were considered and simulated: a grid-connected mode and a stand-alone mode. In grid-connected mode, the main grid is assumed to supply power, allowing the microgrid system to meet load demand at whatever moment and to be aware of power quality at PCC. In stand-alone mode, demand side management is taken into account to balance power, which means the load is modeled based on interrupt mode and interrupt time constraints. In both of two cases, there is a high penetration level (more than 40% generation of total demand) of non-dispatchable DG units with a larger power fluctuation.

A. Grid-Connected Mode

In this mode, the total load of the system is met by the DG units, the ESS and the main grid. The generation supplied by non-dispatchable DG units, dispatchable DG units, main grid are 43.5%, 45.0%, 11.5% of load demand and the network loss is 3.0% as shown in Fig. 7. The microgrid is self-sufficient to meet

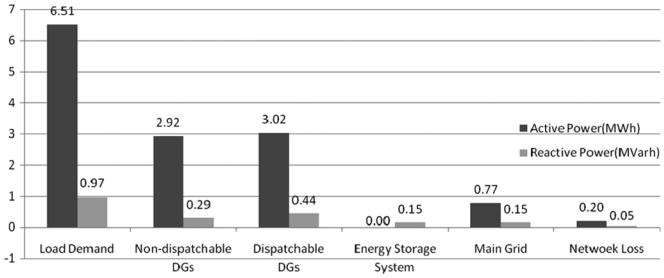

Fig. 7. Generation supply scheme in grid-connected mode.

load demand and almost half of generation comes from renewable sources. The total cost of demand is ¥7644.4 for all power supplied by the main grid. The power from the PV and WT meet most load demand, the cost can be cut down to ¥3987.4. With cooperation of the battery and other DG units, the cost is reduced to ¥3307.8 through the control sequence determined by the schedule layer. It is further reduced to ¥2962.6 by optimizing power flow in the dispatch layer.

Except the economic benefit, performance of the microgrid system is important, too. The schedule layer ensures that the microgrid operates at peak performance, with cooperation of each component over a long time scale, as shown in Fig. 8. During a forecast horizon when market price is low, the microgrid system purchases electricity from the main grid; when the price is high, the microgrid system sells power to the main grid. The market prices have a strong influence on the operation of microgrid; i.e., the microgrid is indirectly controlled by market. On the other hand, this mode maximizes revenues by making use of the price difference with the help of battery storage to shift the power from the main grid through the rule of "buy low, sell high". The power shift from hour 15 to hour 18 using the battery is not only for use with the main grid, but also for use with DG units such as the MT and DE units to ensure these units operate most reliably and economically.

The security and stability of the microgrid is another one of the concerns in energy management, including transmission power, power factor of PCC and voltage, which is ensured by the dispatch layer following the control sequence. The variation range of power factor is $0.98 \sim 1.00$ in PCC. The reactive power is balanced locally in microgrid. It is divided evenly by ESS, non-dispatchable DG units, dispatchable DG units and the main grid. As shown in Fig. 9, the voltages of dispatchable DG units, ESS and PCC change in safe range ($\pm 10\%$).

Due to forecasting error, reserve power is allocated to smooth power fluctuation in dispatch layer as shown in Fig. 10. These are the output of PV, WT, MT, DE and BS from the bottom up, the exchanged power with the main grid and the load during the period 20:00 to 20:30. The practical output of non-dispatchable units fluctuates wildly, relative to smooth predicted value. Owning to schedule layer, DE and MT work in a steady state. At 20:15, the output of WT decreases more than 12 kW relative to predicted value, so FC and BS increase their output to meet power shortage. At next moment, the output of WT increases more than 40 kW, FC and BS reduced their output accordingly. The overall trend of power regulation is growth movement due to the network loss by considering power flow.

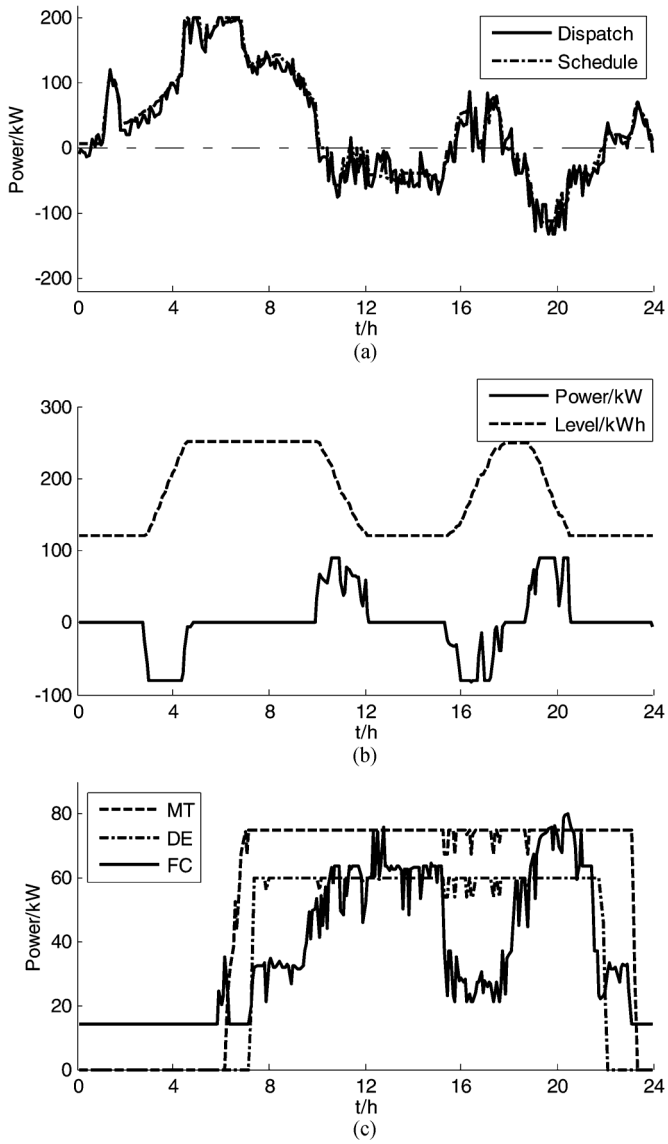

Fig. 8. Operational scheme in grid-connected mode. (a) Power exchanged with the main grid. (b) Energy level and output of the battery. (c) Power of the MT, DE, and FC units.

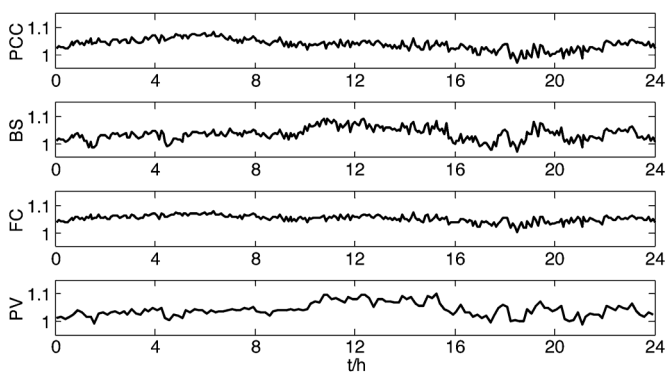

Fig. 9. Voltage magnitude in grid-connected mode (p.u.).

The large forecasting error from 20:15 to 20:20 causes the power de-allocation a few times as shown in Fig. 10(c). The normal deviation limits within 10%. Then increasing the

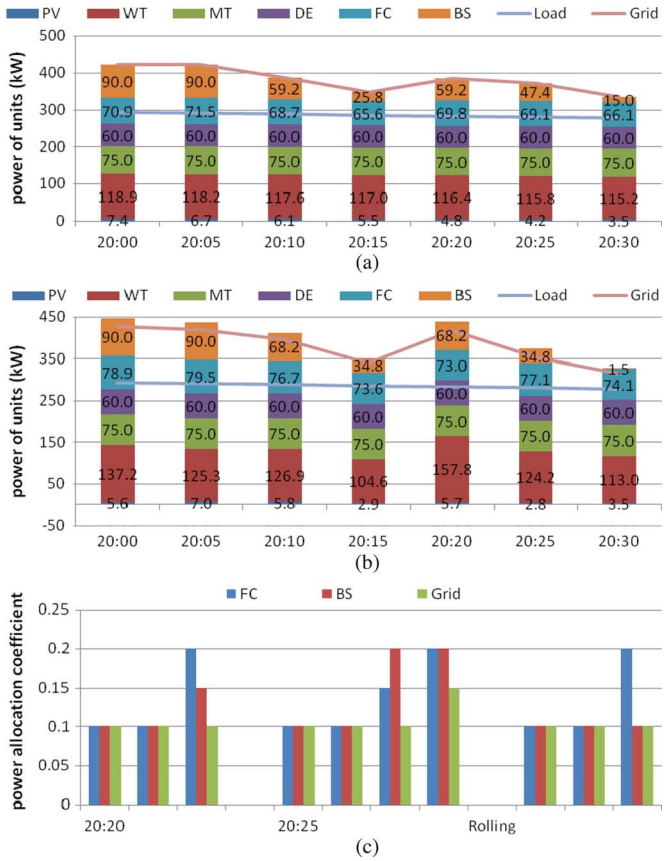

Fig. 10. Operational scheme from 20:00 to 20:30. (a) Operational scheme of schedule layer. (b) Operational scheme of dispatch layer. (c) Power allocation by coordination of the two layers.

penalty factor is used to follow the planned value in second attempt. Next, the power allocation coefficient/deviation limit would be expanded gradually according to incremental cost and adjustable margin. For there is little adjustable margin of DE and MT, FC makes the biggest contribution. As indicated earlier, controllable units would reach their output/energy limit before the planned value due to network loss. A rolling of schedule layer with present working conditions and future information is used to update the rest of operation scheme at 20:20 for reaching the energy level of BS.

More cases are studied with different forecasting error and reserve power (see Table II). Under 5% variance of forecast, the maximum positive/negative deviation is more than 40 kW (>20% of nominal power), and it is more than 60 kW (>30% of nominal power) under 10% variance of forecast. With increase of forecasting error, the calculation increases as coordination and self-adjustment of two layers considering technical and economic aspects. Enlarging the reserve power contributes to decreased calculation and improved convergence, but it increases operation cost for larger reserve power.

B. Stand-Alone Mode

In the long-time operation in stand-alone mode, demand side management should be considered in energy management. In the previous research, traditional loads in Feeder 3 will be cut off and sensitive loads in Feeders 1 and 2 are served as an intentional island under uninterruptible power supply by DG units in stand-alone mode [25]. But power demand of traditional loads is large and important, too. So the approach presented in this paper ensures that power supply to traditional load lasts as long as allowed which means a load shedding is allowed when the power shortage is over the regulation of generation units, but it is tried to be avoided.

TABLE II
RESULTS WITH DIFFERENT FORECAST ERROR IN GRID-CONNECTED MODE

Wind Energy			Photovoltaic Energy			Reserve Power	Number of Calls		Revenue
VF	PD	ND	VF	PD	ND		SL	DL	/¥
0%	—	—	0%	—	—	5%	2	312	4684.0
5%	47.7	47.1	5%	40.5	44.2	5%	4	339	4681.8
						10%	3	333	4681.4
						15%	3	322	4511.8
10%	65.1	60.5	5%	40.5	44.2	10%	7	439	4747.6
						15%	3	423	4498.0
10%	65.1	60.5	10%	74.1	66.0	15%	7	457	4561.5

Note: VF, variance of forecast; PD, maximum positive deviation (kW); ND, maximum negative deviations (kW); SL, schedule layer; DL, dispatch layer.

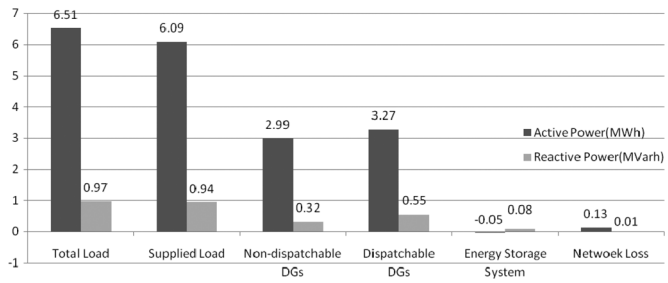

Fig. 11. Generation supply scheme in stand-alone mode.

The generation supplied by non-dispatchable DG units, dispatchable DG units are 48.0%, 52.7% of supplied load and 0.7% of that is stored in battery as shown in Fig. 11. The network loss is 2.1%. As a result, 93.9% of load demand is supplied including 100% of sensitive load and 71.2% of traditional load.

The peak load is 393.7 kW which occurs at about hour 8 in Fig. 12(a) and the capacity of all units in microgrid is 215 kW, so the load cannot be totally met in stand-alone mode. Load shedding gives another mean to balance power. In the schedule layer, part of load is planned to shed that is unsatisfied load such as hour 6 to hour 12. While in the dispatch layer, a little load is shed for power balance such as hour 12 to hour 20 as shown in Fig. 12(b). The unsatisfied load is about 60 kW for the peak load is 335.2 kW after load shedding. If the unsatisfied load is met, another generation unit is needed which only operates in stand-alone mode.

To meet the peak load, MT and DE start up earlier than in the grid-connected mode and gradually climb to normal power in period hour 0 to hour 4 with excess power stored in BS as shown in Fig. 13.

Without support of the main grid, the system voltage is regulated by ESS and dispatchable DG units. Load shedding has little influence on voltage, and the variation caused by non-dispatchable DG units is still controlled in safe range (±10%) as shown in Fig. 14.

More cases are studied with different forecasting error (see Table III). Due to the limit of power output, reserve power is less

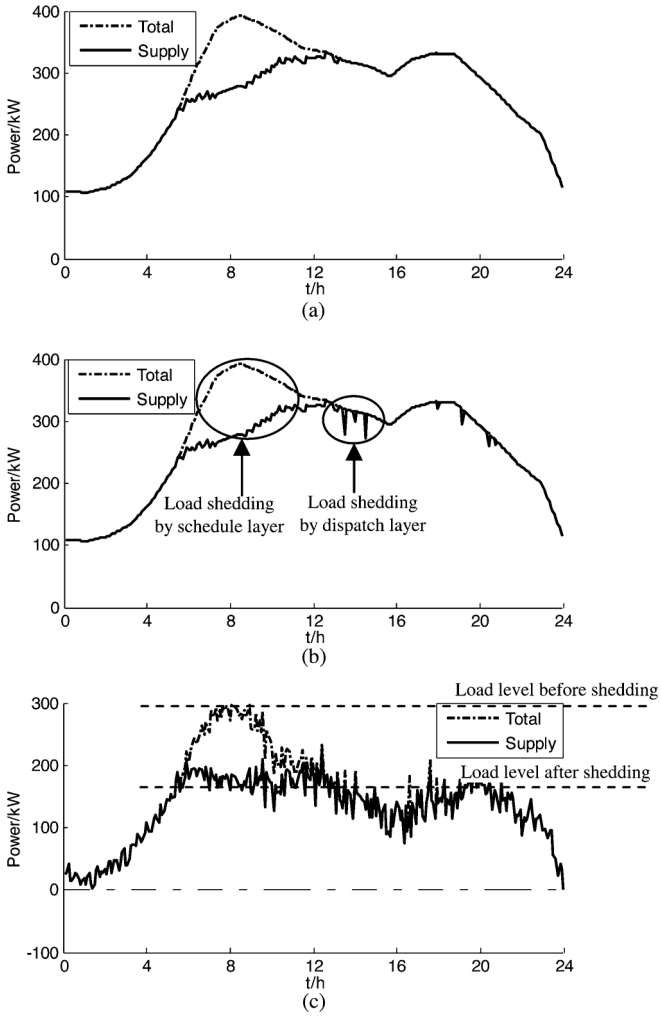

Fig. 12. Load curve in stand-alone mode. (a) Load curve with small forecast error. (b) Load curve with large forecast error. (c) Net load.

than 10% that limits the power regulation of DG units. With increasing forecasting error, satisfaction rate of load decreases. But it keeps above 93% and has a little influence on operation cost.

V. Conclusions

A novel double-layer coordinated control approach for microgrid energy management was proposed in this paper. The proposed approach emphasizes on the difference of grid-connected mode and stand-alone mode, and has good convergence in either mode. The approach allows the microgrid to operate economically, safely and stably by:

1) Considering the influence on the main grid, it maximizes revenues according to DG bids and market price in grid-connected mode with total load supplied and total renewable sources used;
2) Taking the reliable power supply instead of economic benefits, it maximizes satisfaction rate of load with minimum operation cost in stand-alone mode;
3) Coordinating controllable units in the long-time period using the schedule layer to optimize microgrid performance and making the best use of intermittent power resources based on forecasting data;

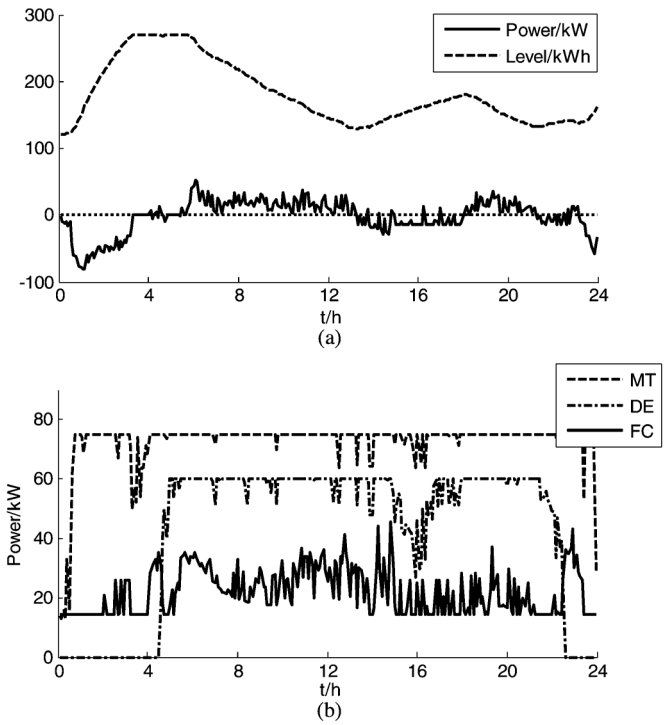

Fig. 13. Operation scheme in stand-alone mode. (a) Energy level and output of the battery. (b) Power of the MT, DE, and FC units.

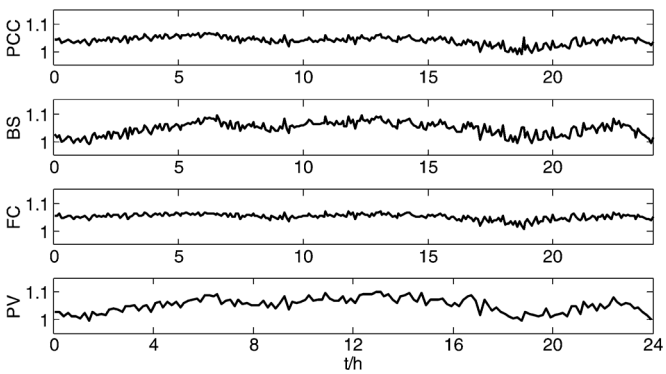

Fig. 14 Voltage magnitude in stand-alone mode (p.u.).

TABLE III
Results With Different Forecast Error in Stand-alone Mode

Variance of forecast		Number of Calls		Max power of load shedding /kW	Peak load after load shedding/kW	Satisfaction rate of load	Cost/ ¥
WT	PV	SL	DL				
0%	0%	3	321	91.3	356.1	95.5%	3186.7
5%	5%	7	382	114.2	335.2	93.9%	3049.4
10%	5%	9	460	114.2	333.8	93.5%	3100.7
10%	10%	14	627	114.2	332.5	92.6%	3055.7

4) Accurately adjusting the generation of units in the real-time layer to optimize power flow and regulating voltage in dispatch layer based on real-time data;
5) Smoothing forecasting error/indeterminacy of uncontrollable units by coordinating the two layers' interact to achieve economic and stability objectives.

REFERENCES

[1] F. Katiraei, R. Iravani, N. Hatziargyriou, and A. Dimeas, "Microgrids management," *IEEE Power Energy Mag.*, vol. 6, no. 3, pp. 54–65, May 2008.

[2] A. L. Dimeas and N. D. Hatziargyriou, "Operation of a multiagent system for microgrid control," *IEEE Trans. Power Syst.*, vol. 20, no. 3, pp. 1447–1455, Aug. 2005.

[3] A. G. Tsikalakis and N. D. Hatziargyriou, "Centralized control for optimizing microgrids operation," *IEEE Trans. Energy Convers.*, vol. 23, no. 1, pp. 241–248, Mar. 2008.

[4] J. A. P. Lopes, C. L. Moreira, and A. G. Madureira, "Defining control strategies for MicroGrids islanded operation," *IEEE Trans. Power Syst.*, vol. 21, no. 2, pp. 916–924, May 2006.

[5] F. Katiraei and M. R. Iravani, "Power management strategies for a microgrid with multiple distributed generation units," *IEEE Trans. Power Syst.*, vol. 21, no. 4, pp. 1821–1831, Nov. 2006.

[6] C. K. Sao and P. W. Lehn, "Control and power management of converter fed microgrids," *IEEE Trans. Power Syst.*, vol. 23, no. 3, pp. 1088–1098, Aug. 2008.

[7] H. Karimi, E. J. Davison, and R. Iravani, "Multivariable servomechanism controller for autonomous operation of a distributed generation unit: Design and performance evaluation," *IEEE Trans. Power Syst.*, vol. 25, no. 2, pp. 853–865, May 2010.

[8] R. Majumder, A. Ghosh, G. Ledwich, and F. Zare, "Power management and power flow control with back-to-back converters in a utility connected microgrid," *IEEE Trans. Power Syst.*, vol. 25, no. 2, pp. 821–834, May 2010.

[9] A. Mehrizi-Sani and R. Iravani, "Potential-function based control of a microgrid in islanded and grid-connected modes," *IEEE Trans. Power Syst.*, vol. 25, no. 4, pp. 1883–1891, Nov. 2010.

[10] C. L. Moreira, F. O. Resende, and J. A. P. Lopes, "Using low voltage MicroGrids for service restoration," *IEEE Trans. Power Syst.*, vol. 22, no. 1, pp. 395–403, Feb. 2010.

[11] G. Diaz, C. Gonzalez-Moran, J. Gomez-Aleixandre, and A. Diez, "Scheduling of droop coefficients for frequency and voltage regulation in isolated microgrids," *IEEE Trans. Power Syst.*, vol. 25, no. 1, pp. 489–496, Feb. 2010.

[12] M. D. Ilic, "From hierarchical to open access electric power systems," *Proc. IEEE*, vol. 95, no. 5, pp. 1060–1084, May 2007.

[13] J. R. Winkelman, J. H. Chow, J. J. Allemong, and P. V. Kokotovic, "Multi-time-scale analysis of a power system," *Automatica*, vol. 16, no. 1, pp. 35–43, Jan. 1980.

[14] C. Sudipta, M. D. Weiss, and M. G. Simoes, "Distributed intelligent energy management system for a single-phase high-frequency AC microgrid," *IEEE Trans. Ind. Electron.*, vol. 54, no. 1, pp. 97–109, Feb. 2007.

[15] H. Kanchev, D. Lu, F. Colas, V. Lazarov, and B. Francois, "Energy management and operational planning of a microgrid with a PV-based active generator for smart grid applications," *IEEE Trans. Ind. Electron.*, vol. 58, no. 10, pp. 4583–4592, Oct. 2011.

[16] E. Sortomme and M. A. El-Sharkawi, "Optimal power flow for a system of microgrids with controllable loads and battery storage," in *Proc. Power Systems Conf. Expo., 2009*, pp. 1–5.

[17] C. Chen, S. Duan, T. Cai, B. Liu, and G. Hu, "Optimal allocation and economic analysis of energy storage system in microgrids," *IEEE Trans. Power Electron.*, vol. 26, no. 10, pp. 2762–2773, Oct. 2011.

[18] D. Zhu, R. Yang, and G. Hug-Glanzmann, "Managing microgrids with intermittent resources: A two-layer multi-step optimal control approach," in *Proc. North American Power Symp., 2010*, pp. 1–8.

[19] G. Hug-Glanzmann, "Coordination of intermittent generation with storage, demand control and conventional energy sources," in *Proc. Bulk Power System Dynamics and Control (iREP)—VIII (iREP), 2010*, pp. 1–7.

[20] L. Wu, M. Shahidehpour, and Y. Fu, "Security-constrained generation and transmission outage scheduling with uncertainties," *IEEE Trans. Power Syst.*, vol. 25, no. 3, pp. 1674–1685, Aug. 2010.

[21] F. A. Mohamed and H. N. Koivo, "System modelling and online optimal management of microgrid using multiobjective optimization," in *Proc. Int. Conf. Clean Electrical Power, 2007*, pp. 148–153.

[22] F. A. Mohamed and H. N. Koivo, "Online management of microgrid with battery storage using multiobjective optimization," in *Proc. Int. Conf. Power Engineering, Energy and Electrical Drives, 2007*, pp. 231–236.

[23] K. Rudion, A. Orths, Z. A. Styczynski, and K. Strunz, "Design of benchmark of medium voltage distribution network for investigation of DG integration," in *Proc. IEEE Power Engineering Society General Meeting, 2006*, 6 pp..

[24] S. H. Karaki, R. B. Chedid, and R. Ramadan, "Probabilistic performance assessment of autonomous solar-wind energy conversion systems," *IEEE Trans. Energy Convers.*, vol. 14, no. 3, pp. 766–772, Sep. 1999.

[25] N. Hatziargyriou, H. Asano, R. Iravani, and C. Marnay, "Microgrids," *IEEE Power Energ. Mag.*, vol. 5, no. 4, pp. 78–94, Jul. 2007.

Quanyuan Jiang (M'10) received the B.S., M.S., and Ph.D. degrees in electrical engineering from Huazhong University of Science & Technology (HUST), Wuhan, China, in 1997, 2000, and 2003, respectively.

He has worked at Zhejiang University (ZJU), Hangzhou, China, as a faculty since July 2003. He is currently a full professor in College of Electrical Engineering, Zhejiang University. His research interests include power system stability and control, optimization, and parallel computing.

Meidong Xue received the B.S. degree in 2010 from Zhejiang University, Hangzhou, China, where he is currently pursuing the Ph.D. degree in electrical engineering.

His research interest includes management of microgrids.

Guangchao Geng (S'10) received the B.S. degree in 2009 from Zhejiang University, Hangzhou, China, where he is currently pursuing the Ph.D. degree in electrical engineering.

His research interest includes power system optimization and parallel computing.